EUROPEAN ORGANIZATION FOR NUCLEAR RESEARCH



# INCLUSIVE $\pi^0$ PRODUCTION FROM HIGH ENERGY P-P COLLISIONS AT VERY LARGE TRANSVERSE MOMENTA

* * *

A.G. Clark, P. Darriulat, P. Dittmann*, K. Eggert**, V. Hungerbühler, P.M. Patel§, J. Strauss§§, and A. Zallo,
CERN, Geneva, Switzerland.

B. Aubert+, M. Banner, J.C. Chèze, C. Lapuyade, T. Modis++, P. Perez, J. Teiger, C. Tur, J.P. Vialle+, H. Zaccone, and A. Zylberstejn,
CEN Saclay, France

P. Jenni, P. Strolin, G.J. Tarnopolsky,
ETH Zürich, Switzerland

## ABSTRACT

We report on measurements of inclusive $\pi^0$ production at c.m. energies of 53 and 63 GeV, $\theta \simeq 90^0$, from p-p collisions at the CERN ISR. In the range $0.2 < x_t < 0.45$ the data can be described by a form :

$$Ed^3\sigma/dp^3 \propto p_t^{-(6.6 \pm 0.8)} (1-x_t)^{(9.6 \pm 1.0)}$$

* Now at DESY, Hamburg, Germany.
** III. Physikalisches Institut der Technischen Hochschule, Aachen, Germany.
§ Visitor from McGill University, Montreal, Canada.
§§ Insitut für Hochenergie Physik der Österr. Akademie der Wissenschaften, Vienna, Austria.
\+ LAL Orsay, France.
++ Now at Université de Genève, Geneva, Switzerland.

## INTRODUCTION

Inclusive production of large transverse momentum pions[1,2,3] in high energy p-p collisions has been extensively studied both at FNAL and at the CERN ISR. Invariant cross sections are observed to obey a scaling law of the form :

$$E \frac{d^3\sigma}{dp^3} \propto p_t^{-n} f(x_t,\theta), \qquad (1)$$

where E and p are the energy and momentum of the secondary, $\theta$ the production angle, $p_t = p \sin\theta$ the transverse momentum and $x_t = 2 p_t / \sqrt{s}$, s being the c.m. energy squared. The exponent n, which in parton models is related to the number of point-like constituents taking an active part in the interaction, is measured to be in the range of 7 to 9, contrasting with the value of n = 4 expected in the absence of any dimension in the basic scattering process.

It is important to compare the data with relation (1) in the largest possible ($p_t$, $x_t$) domain. We report on measurements of inclusive $\pi^0$ production at the highest ISR energies ($\sqrt{s}$ = 53 an 63 GeV) and at $\theta \simeq 90^0$, which extend the explored range of $x_t$ by a factor of two, from $x_t < 0.25$ to $x_t < 0.5$.

## THE DETECTOR

The detector is a large solid-angle double arm spectrometer of a design optimized for highly selective electron identification. Each arm covers a solid angle of the order of 0.6 sr around $\theta = 90^0$. When following its elements outward from the interaction region (Fig. 1), one finds :

i) a double layer hodoscope, with 8 scintillators per layer,

ii) a set of seven drift chambers,

iii) a 12-cell atmospheric-pressure air Cerenkov counter embedded in the gap of an analyzing magnet,

iv) another set of drift chambers,

v) a scintillator-iron-scintillator sandwich hodoscope segmented in twenty vertical strips,

vi) an array of 138 lead glass cells, each of 14 radiation lengths.

In the present work we shall consider almost exclusively the lead glass arrays, which are used to detect photons from $\pi^0$ decays and to measure their energies. However the rest of the detector is essential to discriminate against background.

Each array consists of 138 lead glass blocks, each at a distance of 2.3 m from the intersection. Each block is equipped with a phototube. Anode pulses are analysed in 10-bit analogue-to-digital converters, while pulses from the last dynode are added for subsequent energy discrimination. The detector is triggered when a signal above threshold in one of the lead glass arrays is recorded in coincidence with a signal from one of the scintillators located near the interaction region. This scintillator signal is used to start the 170 ns wide gate over which anode pulse integration is performed.

The calibration of the energy response of the detector is of crucial importance since the measured spectra are rapidly decreasing functions of $p_t$. Before installation, each block was calibrated in a 2 GeV electron beam at the CERN-PS and its phototube voltage was adjusted to ensure a uniform gain over the full array. This calibration was maintained throughout the experiment by means of reference light sources ($^{241}$Am deposited on a small plastic scintillator which was glued to the front face of each block). To obtain a response similar to that of a 1.5 GeV photon, the anode pulses were amplified by a factor of 10 during calibration. The gain and linearity of each amplifier were known from a separate measurement. In addition the lead glass arrays were periodically recessed to 4 m from the intersection, at which distance $\pi^0 \to \gamma\gamma$ decays yield two spatially resolved photons. Data collected in this configuration enable a check of the calibration of each cell to within ±5% for photon energies between 0.5 and 2 GeV. The energy-loss in the iron-scintillator sandwich is also evaluated from these data ($\sim$ 30 MeV per minimum ionizing pulse-height in the back scintillators). Using in addition a set of 1000 $J/\psi \to e^+e^-$ decays in which the electrons are detected in opposite arms, we estimate an uncertainty of ±3% on the energy measurement in the 1-2 GeV range. The energy resolution, including uncertainties on the

absolute cell to cell calibration, is found to have the form :

$$\frac{\Delta E}{E} = \pm \left\{ (.05)^2 + \frac{(.11)^2}{E(GeV)} \right\}^{\frac{1}{2}}$$

The linearity of the energy response to electrons between 2 and 12 GeV was measured at the CERN PS both for normal and $34^0$ incidence. It was corroborated to within 2%. Small deviations from linearity at low pulse height, occuring at the input stage of the analogue to digital converters, have been measured with standard pulses and corrected.

## DATA REDUCTION

For each event, the pattern of energy deposition in the lead glass array is analysed and reduced to a number of clusters. Each cluster is defined as a set of adjacent cells having energies above 100 MeV. When necessary a halo contribution from surrounding cells is added to its energy. When the energy distribution within a cluster is observed to peak in two non-adjacent cells,.the cluster is split in two different sub-clusters. Two photon-clusters can be resolved down to a 30 cm separation between photons. In the high energy range of the experiment the photons from $\pi^0$ decays are mostly unresolved : at 6 GeV, a $\pi^0$ yields two resolved photons only 6% of the time, and then the leading photon carries more than 97% of the total $\pi^0$ energy.

In principle it is sufficient to select events with an energy cluster above trigger threshold. In doing so we have accounted for the fact that different runs were taken with different thresholds, as well as for small possible threshold differences in different branches of the trigger electronics.

However, such a sample is contaminated by two kinds of background :
i) events not associated to beam-beam interactions,
ii) energy clusters induced from secondaries other than $\pi^0$'s.
Backgrounds of the first kind include spurious phototube pulses, beam halo interactions and cosmic rays.

Large spurious phototube pulses are observed to occur in a small number ($\sim$5%) of cells at a rate of a few per minute and with a uniform

pulse height distribution. They are only partially eliminated on-line by the requirement of a coincidence with one of the front scintillators because of the large resolving time ($\sim$100 ns) and of the high scintillator rate ($\sim$200 kHz). In order to suppress this background to a negligible level we reject single-cell clusters by requiring that not more than 90% of the cluster energy be contained in a single cell. We have checked the effectiveness of this procedure on a sample of beam-off triggers where the scintillator-coincidence requirement was omitted. The fraction of real $\pi^0$'s thus rejected has been evaluated by means of a detailed calculation parametrizing the development of a photon shower within the lead glass. The parameters entering this calculation were adjusted on well identified electrons (from $J/\psi \to e^+e^-$) and photons (from resolved $\pi^0 \to \gamma\gamma$). The energy dependence of the shower length was taken from the model of Longo and Sestili [4] and checked against the results of our 12 GeV electron calibration data. The loss of real $\pi^0$'s is found to increase from 11% at $p_t$ = 6 GeV/c to 29% at $p_t$ = 13 GeV/c and has been accounted for.

Beam-gas interactions produce a halo of high-energy forward-collimated secondaries which occasionally induce long horizontal clusters in the lead-glass arrays. They are eliminated by rejecting clusters extending over more than four columns or having energy in one of the edge columns. The cosmic-ray background has been measured in periods when the beams were off. It was observed to be mostly associated to large showers. It is strongly suppressed once we require that no charged track should point to the energy cluster, that the upper and lower rows should contain less than 10% of the cluster energy, and that the cluster should not extend over more than three rows. However, because of its slowly decreasing energy spectrum, it remains important at very large values of $p_t$.

Backgrounds of the second kind, namely associated to a beam-beam collision, include occasional large energy depositions from charged or neutral hadrons, possible direct photons, and the radiative decay of particles other than $\pi^0$.

The thickness of the lead glass arrays corresponds to approximately 2 collision lengths, which is usually too small to fully contain a hadron shower. A hadron may however interact in the glass and produce sufficiently

energetic $\pi^0$'s to deposit a substantial fraction of its energy. Anti-nucleons annihilating in the lead glass may produce an apparent energy larger than their own.

The requirement that no charged track should point to the energy cluster provides a straightforward rejection of charged hadrons. Neutrons, antineutrons and neutral kaons cannot be so simply eliminated. Their contribution is estimated from a study of the lead glass response to charged hadrons, making use of momentum measurement in the magnetic spectrometers. A strong excess of negative charges, which we attribute to antiprotons, is observed with momenta between 1 and 3.5 GeV/c, corresponding to apparent lead glass energies up to 4.5 GeV. Above 6 GeV, their contribution is observed to be negligible. In this range the fraction of clusters associated to a track is of the order of 10%, approximately independent upon energy. Under the assumption that at least half of these correspond to charged pions, we estimate that the neutral hadron background contribution does not exceed 5%. An independent estimate is obtained from a study of the conversion probability in the iron-scintillator sandwich for a subsample of relatively isolated clusters (to ensure an unambiguous association with the sandwich scintillators). The single photon conversion probability used as reference is measured from resolved $\pi^0 \to \gamma\gamma$ decays to be 56 ± 2%, corresponding to a radiation length in iron of 1.8 cm. The conversion probability is found lower than expected for guenuine $\pi^0$'s and corresponds to a 10% contamination of neutral hadrons. Alternatively, retaining our former 5% estimate, it corresponds to an additional 10% contamination of single photons and leads to a total correction of (15 ± 7)%.

The contribution of $\eta \to \gamma\gamma$ decays is strongly suppressed by the cut on cluster size which is applied to reduce backgrounds not associated to beam-beam interactions. This is confirmed by a comparison between the observed rms cluster radius distributions and the result of a calculation combining $\pi^0$, $\eta$ decay kinematics and shower development in the glass.

Finally corrections were applied to account for $\pi^0$'s which enter the lead glass arrays at a small distance from another particle, thus forming overlapping clusters. When rejecting clusters to which a track is observed to point, nearby genuine $\pi^0$'s are rejected. This introduces a loss of 2%, approximately energy-independent, which was evaluated by

extrapolation from a sample of neighbouring track-cluster pairs under the assumption of the absence of a super-short range component in the two-particle correlation function. A similar procedure was applied to pairs of nearby clusters to obtain the correction for the occasional overlap of two $\pi^0$'s. These clusters do not, in general, fullfill the condition of extending over less than 4 cells horizontally and 3 cells vertically. This leads again to a 2%, energy independent, loss. However, when two $\pi^0$'s, or a $\pi^0$ and a spurious single cell cluster, happen to be close enough, they may merge into a cluster sufficiently small to be accepted, but with an overestimated energy. This correction, evaluated by the same extrapolation procedure, is observed to increase from 4% at $p_t$ = 5 GeV/c to 20% at $p_t$ = 12 GeV/c.

A summary of the various corrections and related uncertainties is given in Table 1.

## RESULTS

Invariant cross sections averaged over a rapidity interval of ± 0.6 units are evaluated from the data using an acceptance calculation taking into account the geometry of the detector and the transformation to the c.m. system of the colliding protons. Relevant luminosities are measured from a coincidence between two telescopes pointing to the interaction region and calibrated by the Van der Meer method [5]. The data have been corrected for the bias introduced by the requirement of a coincidence with one of the front scintillators. This correction, evaluated from a study of the scintillator multiplicity distribution, decreases from 15% at $p_t$ = 6 GeV/c to 8% at $p_t$ = 15 GeV/c. We have checked for internal consistency between runs taken with equal trigger thresholds and between subsets of data corresponding to different branches of the trigger electronics within the same run. In particular we have verified that both spectrometer arms yield equal cross sections to within 6%.

By combining the effects of these various uncertainties we evaluate a global uncertainty of ± 17% on the absolute normalization (Table 1). When integrated over $p_t$ from 6 GeV/c onwards, invariant cross sections exibit no significant dependence upon rapidity to within 15%.

The results are listed in Table 2. The smearing due to the finite energy resolution has been unfolded. Invariant cross sections are displayed in Figure 2 versus $x_t$. In this representation they are expected to exhibit the same dependence upon $x_t$ at different values of $\sqrt{s}$ if relation (1) is valid, and their relative normalization provides a direct measure of n. We have attempted to fit the data to a form :

$$Ed^3\sigma/\,dp^3 = Ap_t^{-n}\,(1-x_t)^m\ ,\ (E,\ p_t \text{ in GeV},\ \sigma \text{ in cm}^2).$$

Good fits are obtained with values of n in the range of 6 to 7, depending upon the $x_t$ interval within which the fit is performed. Within errors we observe no significant dependence of n upon $x_t$. In the range $0.2 < x_t < 0.45$ we find $A = (55 \pm 15)\ 10^{-29}$, $n = 6.6 \pm 0.8$ and $m = 9.6 \pm 1.0$ with a $\chi^2$ of 17 for 17 degrees of freedom. While A and m are strongly correlated parameters, n is defined without ambiguity from the ratio of the cross sections measured at both values of $\sqrt{s}$.

When compared to the Fermilab data on charged pions[3] in the same range of $x_t$ ( $n \simeq 8.2$ to 8.5, $m \simeq 9.0$ to 9.9) this result indicates a decrease of n, the $x_t$ dependence not being significantly affected. A similar observation[2] had already been made in a lower $x_t$ region at the highest ISR energies. In the interval $0.2 < x_t < 0.4$ the ratio between the average 400 GeV charged pion cross sections[3] and the present data corresponds to $n = 7.3 \pm 0.6$.

ACKNOWLEDGEMENTS

We have benefitted, at various stages of the experiment, from the contributions of Drs. C. Alff-Steinberger, H.R. Renshall, and K. Zalewski. The technical assistance of H. Acounis, G. Bertalmio, L. Bonnefoy, J.M. Chappuis, C. Engster, M. Lemoine, L. McCulloch, J.C. Michaud and A. Mottet is gratefully acknowledged. We wish to thank Dr H. Hoffmann for help in installing the experiment at the ISR and Drs L. Di Lella, J. Mayer and A. Wetherell for permission to use part of their installation at the CERN-PS for lead glass calibration.

REFERENCES

1 - F.W. Büsser et al., Nucl. Phys. B 106 (1976) 1.

2 - K. Eggert et al., Nucl. Phys. B 98 (1975) 49.

3 - D. Antreasyan et al., Phys. Rev. Lett. 38 (1977) 112.

4 - E. Longo and I. Sestili, Nucl. Inst. 128 (1975) 283.

5 - S. Van der Meer, CERN-ISR-PO/68-31 (June 1968) unpublished.

TABLE I

Summary of corrections and uncertainties
(in percent)

| I - Momentum dependent quantities | $p_t$ = 6 GeV/c | $p_t$ = 12 GeV/c |
|---|---|---|
| Single cell rejection | +12 ± 3 | +37 ± 6 |
| Neutral hadrons/single photons | -15 ± 7 | -15 ± 7 |
| Overlaps (charged) | + 2 ± 2 | + 2 ± 2 |
| Overlaps (neutrals) | - 3 ± 3 | -18 ± 10 |
| Photon conversions (vacuum pipe, etc...) | + 4 ± 1 | + 4 ± 1 |
| Background (cosmics, beam gas..) | 0 | -28 ± 14 |
| Smearing (finite resolution) | -11 ± 4 | -29 ± 10 |
| Front scintillator coincidence | +17 ± 5 | + 9 ± 3 |
| | + 2 ± 11 | -45 ± 22 |

| II - Absolute normalization | |
|---|---|
| Monitor constants | ± 5 |
| Internal consistency | ± 15 |
| Acceptance calculation | ± 7 |
| | ± 17 |

| III - Energy scale | |
|---|---|
| Global scale error | ± 3 |
| Uncertainty on linearity | ± 2 |

TABLE 2

Invariant cross sections for inclusive $\pi^0$ production. Quoted uncertainties include statistical errors and $p_t$ dependent systematic uncertainties.

| $\sqrt{s}$ = 53 GeV | | $\sqrt{s}$ = 63 GeV | |
|---|---|---|---|
| $p_t$ (GeV/c) | $Ed^3\sigma/dp^3$ ($cm^2$ $GeV^{-2}c^3$) | $p_t$ (GeV/c) | $Ed^3\sigma/dp^3$ ($cm^2$ $GeV^{-2}c^3$) |
| 5.25 | $(.85 \pm .12)\ 10^{-33}$ | 5.25 | $(.19 \pm .03)\ 10^{-32}$ |
| 5.75 | $.45 \pm .06$ | 5.74 | $.09 \pm .01$ |
| 6.24 | $.19 \pm .03$ | 6.23 | $(.46 \pm .06)\ 10^{-33}$ |
| 6.73 | $.12 \pm .02$ | 6.72 | $.22 \pm .03$ |
| 7.24 | $(.60 \pm .08)\ 10^{-34}$ | 7.23 | $.12 \pm .02$ |
| 7.72 | $.30 \pm .04$ | 7.72 | $(.63 \pm .09)\ 10^{-34}$ |
| 8.22 | $.16 \pm .03$ | 8.23 | $.31 \pm .05$ |
| 8.74 | $(.86 \pm .14)\ 10^{-35}$ | 8.72 | $.17 \pm .03$ |
| 9.23 | $.49 \pm .09$ | 9.21 | $(.88 \pm .18)\ 10^{-35}$ |
| 9.76 | $.29 \pm .07$ | 9.72 | $.40 \pm .11$ |
| 10.40 | $.10 \pm .03$ | 10.34 | $.19 \pm .06$ |
| 11.41 | $(.36 \pm .16)\ 10^{-36}$ | 11.48 | $(.79 \pm .37)\ 10^{-36}$ |
| 12.53 | $.15 \pm .10$ | 12.29 | $.15 \pm .14$ |
| 13.32 | $(.29\ ^{+.49}_{-.29})\ 10^{-37}$ | 13.13 | $(.24\ ^{+.64}_{-.24})\ 10^{-37}$ |
| 14.32 | $.10\ ^{+.35}_{-.10}$ | 14.61 | $.26\ ^{+.98}_{-.26}$ |
| 15.34 | $.03\ ^{+.31}_{-.03}$ | 15.69 | $.05\ ^{+.59}_{-.05}$ |
| 16.39 | $.01\ ^{+.12}_{-.01}$ | 16.51 | $.01\ ^{+.38}_{-.01}$ |

FIGURE CAPTIONS

1 - Exploded view of one of the spectrometer arms.

2 - Invariant cross section for inclusive $\pi^0$ production at $\sqrt{s}$ = 53 GeV (open circles) and $\sqrt{s}$ = 63 GeV (full dots) as a function of $x_t$. Data from references 1 and 2 are indicated as a cross-hatched band. Also shown (triangles) are the data from Ref. 3 averaged betwen $\pi^+$ and $\pi^-$ production. The lines are the result of the best fit to relation (1).

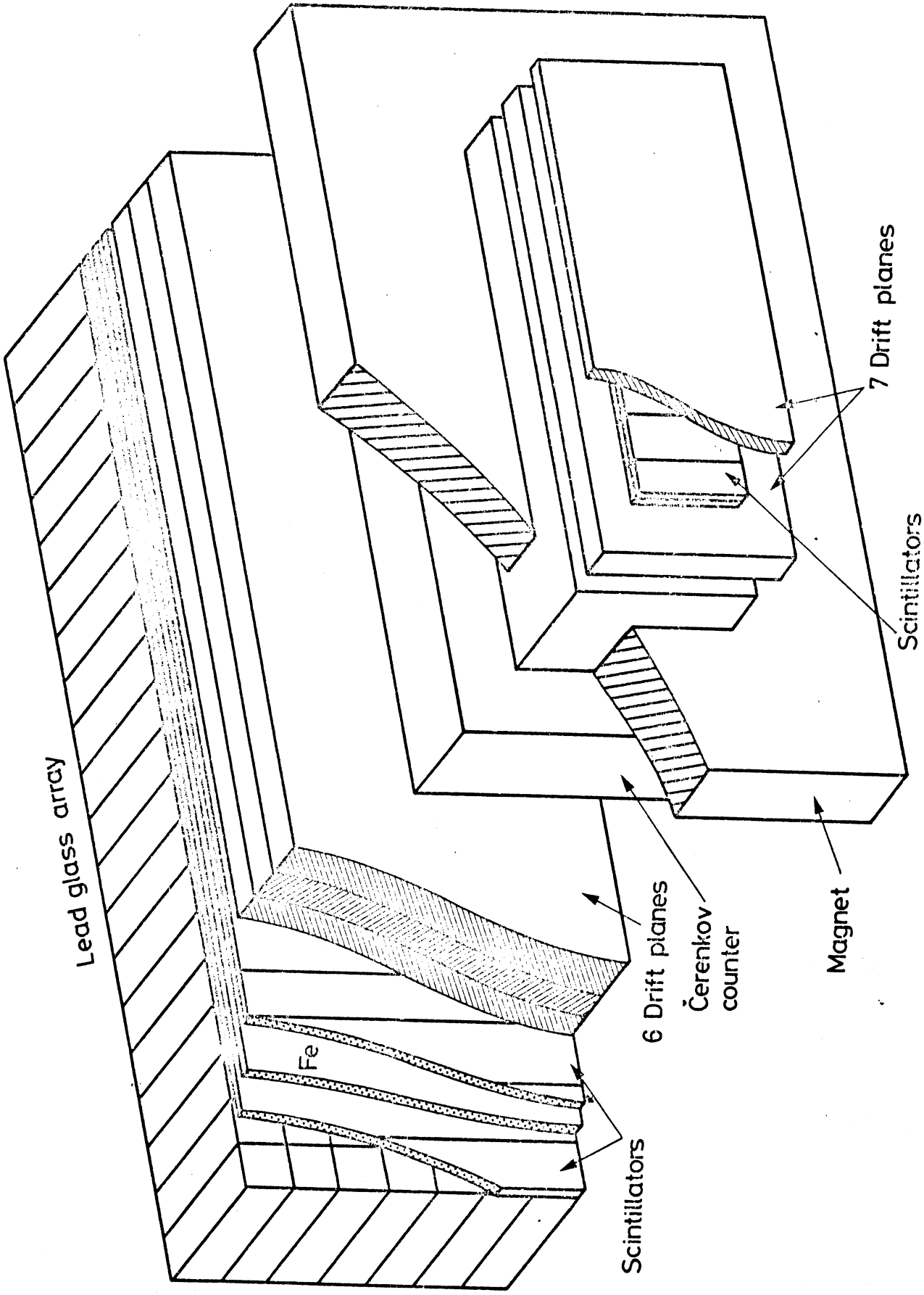
Lead glass array
Fe
Scintillators
6 Drift planes
Čerenkov counter
Magnet
7 Drift planes
Scintillators

Figure 1

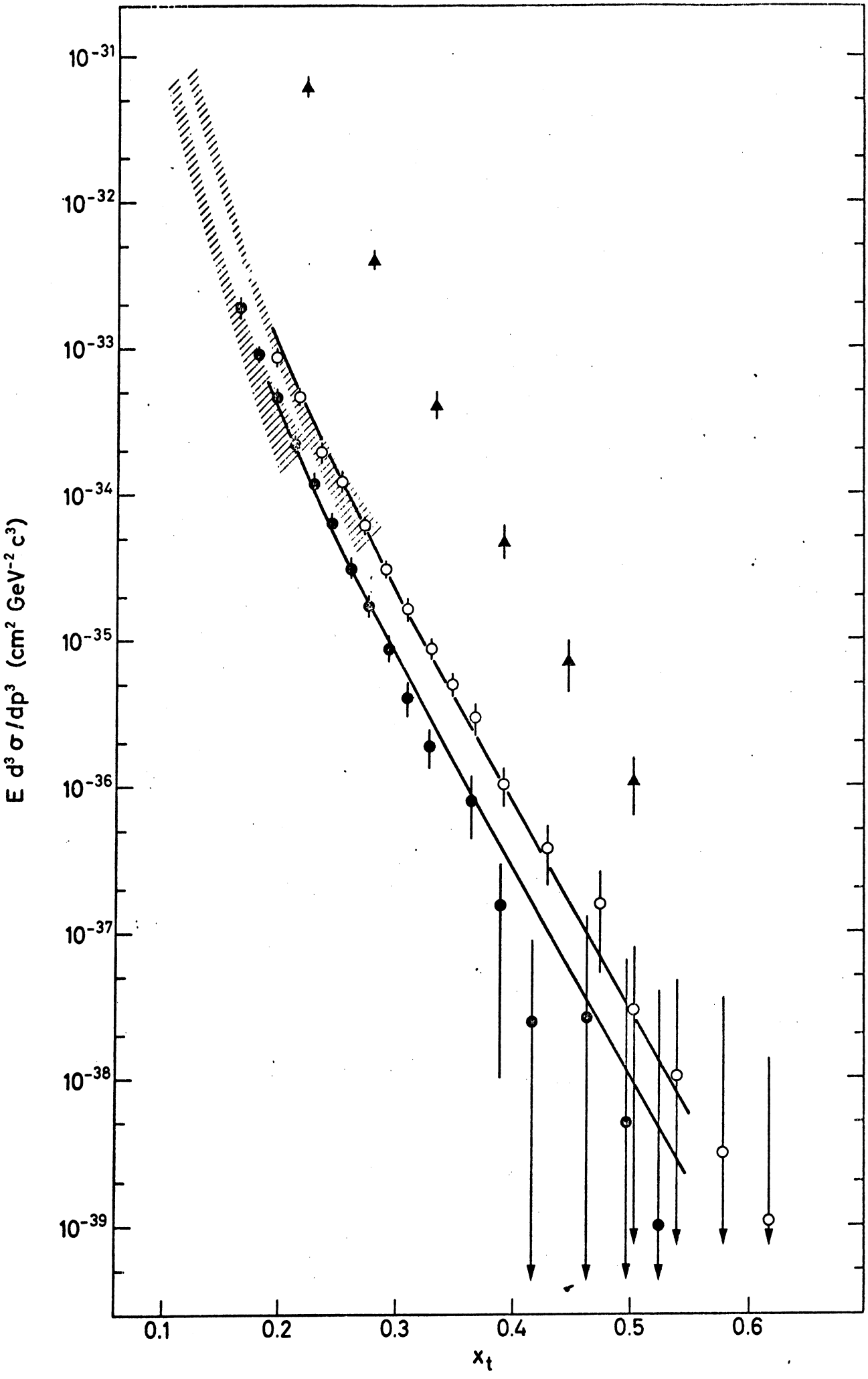
$10^{-31}$
$10^{-32}$
$10^{-33}$
$10^{-34}$
$10^{-35}$
$10^{-36}$
$10^{-37}$
$10^{-38}$
$10^{-39}$
E $d^3\sigma/dp^3$ (cm$^2$ GeV$^{-2}$ c$^3$)
0.1
0.2
0.3
0.4
0.5
0.6
$x_t$

Figure 2